3

Guidance of *Drosophila* mushroom body axons depends upon DRL-Wnt receptor cleavage in an adjacent brain structure

Elodie Reynaud[1] , Liza L. Lahaye[2] , Ana Boulanger[1] , Iveta M. Petrova[2] , Claire Marquilly[1] , Adrien Flandre[1] , Tania Martianez[2] , Martin Privat[1] , Jasprina N. Noordermeer[2] , Lee G. Fradkin[2] * and Jean-Maurice Dura[1] *

1 Institute of Human Genetics, UPR1142, CNRS, 141, rue de la Cardonille, 34396 Montpellier, France.
2 Department of Molecular Cell Biology, Leiden University Medical Center, Leiden, The Netherlands.
* Corresponding authors. E-mail: jean-maurice.dura@igh.cnrs.fr ; L.G.Fradkin@lumc.nl

Accepted manuscript posted online 26 August 2013, doi: 10.1128/MCB.00169-13
Mol. Cell. Biol. October 2013 vol. 33 no. 20 4116-4127

SUMMARY

In vivo axon pathfinding mechanisms in the neuron-dense brain remain relatively poorly characterized. We study the *Drosophila* mushroom body (MB) axons whose α and β branches connect to different brain areas. We show that the Ryk family WNT5 receptor, DRL (derailed) which is expressed in the dorsomedial lineages, brain structure precursors adjacent to the MBs, is required for MB α branch axon guidance. DRL acts to capture and present WNT5 to MB axons rather than transduce a WNT5 signal. DRL's ectodomain must be cleaved and shed to guide α axons. DRL-2, another Ryk, is expressed within MB axons and functions as a repulsive WNT5 signaling receptor. Finally, our biochemical data support the existence of a ternary complex composed of the cleaved DRL ectodomain, WNT5 and DRL- 2. Thus, the interaction of MB-extrinsic and -intrinsic Ryks via their common ligand acts to guide MB α axons.

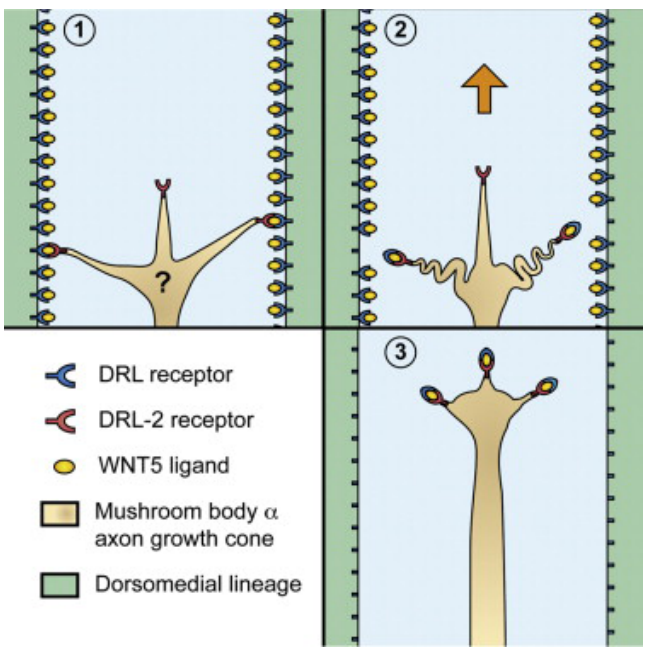

INTRODUCTION

The MBs are structures in the insect brain implicated in learning and memory (reviewed in Heisenberg, 2003). Each MB arises from 4 neuroblasts which give rise sequentially to three types of neurons: γ neurons (late embryonic and early larval stage), α'β' neurons (late larval stage) and αβ neurons (pupal stage). Each αβ neuron projects an axon that branches to send an α branch dorsally, which contributes to the formation of the α lobe, and a β branch medially, which contributes to the formation of the β lobe (Lee et al., 1999). The α lobe plays specific roles in long-term aversive memory in the *Drosophila* adult brain (Pascual and Preat, 2001; Yu et al., 2006). Different guidance cues are likely required for the α and β branches. For instance, mutations in the *Eph* and *Hiw* genes result in specific effects on α branch versus β branch guidance, respectively (Boyle et al., 2006; Shin and DiAntonio, 2011). The *drl* gene encodes a receptor tyrosine kinase-related protein, which plays roles with its ligand WNT5 in MB development and was first isolated on its role in olfactory memory (Dura et al., 1993; Grillenzoni et al., 2007).

drl' s first described role in axon guidance was axon commissure choice in the embryonic nerve cord (Bonkowsky et al., 1999; Callahan et al., 1995; Yoshikawa et al., 2003). Each ventral nerve cord segment has two commissures, one anterior and one posterior, where the axons that project contra-laterally cross the midline. The *drl*$^{+}$ expressing neurons send their axons in the anterior commissure because of the presence of WNT5, a repulsive ligand, in the posterior commissure. Here, we report that *drl* is required during brain development for MB α branch guidance, but a lack of DRL does not affect branching of the αβ axons. We confirm our previous report (Grillenzoni et al., 2007) that *drl* is neither expressed nor required within the αβ neurons and demonstrate that, rather, it is expressed by a neural cell lineage adjacent to, but distinct from, the extending MB axons. Interestingly, DRL's cytoplasmic domain, and hence its intracellular signaling activity, is not required for correct α axon guidance. The cytoplasmic domain of another Ryk, DRL-2 which is expressed by MB neurons, is however required for α axon guidance indicating that it acts as an MB axon-intrinsic WNT5 receptor. Furthermore, we demonstrate that DRL's conserved putative tetrabasic cleavage (TBC) site, whose cleavage results in the extracellular shedding of DRL's Wnt-binding domain, is required for MB axon guidance. Finally, we find that the shed DRL extracellular domain forms a complex, via WNT5, with transmembrane DRL-2. Our data indicate a novel mechanism regulating Wnt signaling where a shed extrinsic receptor serves to guide brain axons.

RESULTS

α axons are misguided in *drl* and *wnt5* mutants

Here, we show that *drl* is required for appropriate MB α axon guidance. By examining visualization MARCM (Lee and Luo, 1999) MB neuron clones in the drl^{null} mutant brain, we found that branching of the α and β branch axons occurs normally but that α axons extend inappropriately along the medial trajectory and display aberrant midline crossing (Figures 1A and 1B). Notably, the separation angle between the wild-type α and β axon branches is still observed in *drl* mutants (wild-type: 118.4° ± 5.7°; *drl*: 128.1° ± 16.6°; P = 0.60; t test, results are means ± s.e.m. with n = 5 in each case) indicating that initial appropriate separation between the branches occurs. We observed abnormal midline crossing previously in drl^{null} mutant MBs (Grillenzoni et al., 2007). These two defects, α axon misguidance and midline crossing, are independent since we found one or the other in *drl* hypomorphs (drl^{hypo}; an incomplete loss-of-function allele) (Figures 1C and 1D and Table S1). In this study we focus on α axons since their trajectory, and not that of the β's, is altered in the *drl* mutant. We scored for axon growth defects where the axon stops soon after the branching point. Notably, we did not observe α axon growth defects in the 36 single- and two-neuron null clones analyzed, but 35 out of these 36 clones (97%) displayed α misguidance (Figure 1G and Table S2). These results demonstrate that the *drl* receptor is required for MB α axon guidance. αβ axons extend individually and asynchronously from newly-born αβ neurons which are derived from continuously dividing neuroblasts for most of the pupal stage (circa 5 days at 25°C). α axon misguidance was observed in drl^{null} animals as soon the adult αβ axons can be visualized with a specific pioneer αβ GAL4 line (*c708a*-GAL4 (Zhu et al., 2006)) (data not shown). The *c708a*-GAL4 was not expressed strongly enough in the early pupae to visualize the pioneer αβ at that stage but the misguidance observed in the adult brain likely reflects earlier guidance errors in the developing brain.

The WNT5 protein acts as a repulsive axon guidance ligand for the DRL receptor in the embryonic central nervous system (Yoshikawa et al., 2003) and is involved in MB development (Grillenzoni et al., 2007). Thus, we evaluated the effects of the loss of *wnt5* on α axon guidance in the MBs. The analysis of *wnt5* mutant brains with *c739*-GAL4 line (Figure S1) revealed absence of α lobe (circa 30% of the MBs), absence of α and β lobe (circa 50% of the MBs) as well as wild-type MBs (circa 20%). If we take into account only where α axons are affected, examination of visualization MARCM clones in $wnt5^{null}$ brains, revealed misguidance in 60% of them (n=20) (Figure 1E) while the remainder had growth defects (Table S2) similarly to what was previously reported (Shimizu et al., 2011). Both α and β guidance were also observed to be affected in the same neurons (Figure S1E and H). Altogether, 51% of the $wnt5^{null}$ clones (n=47) displayed α axon misguidance (Figure 1G and

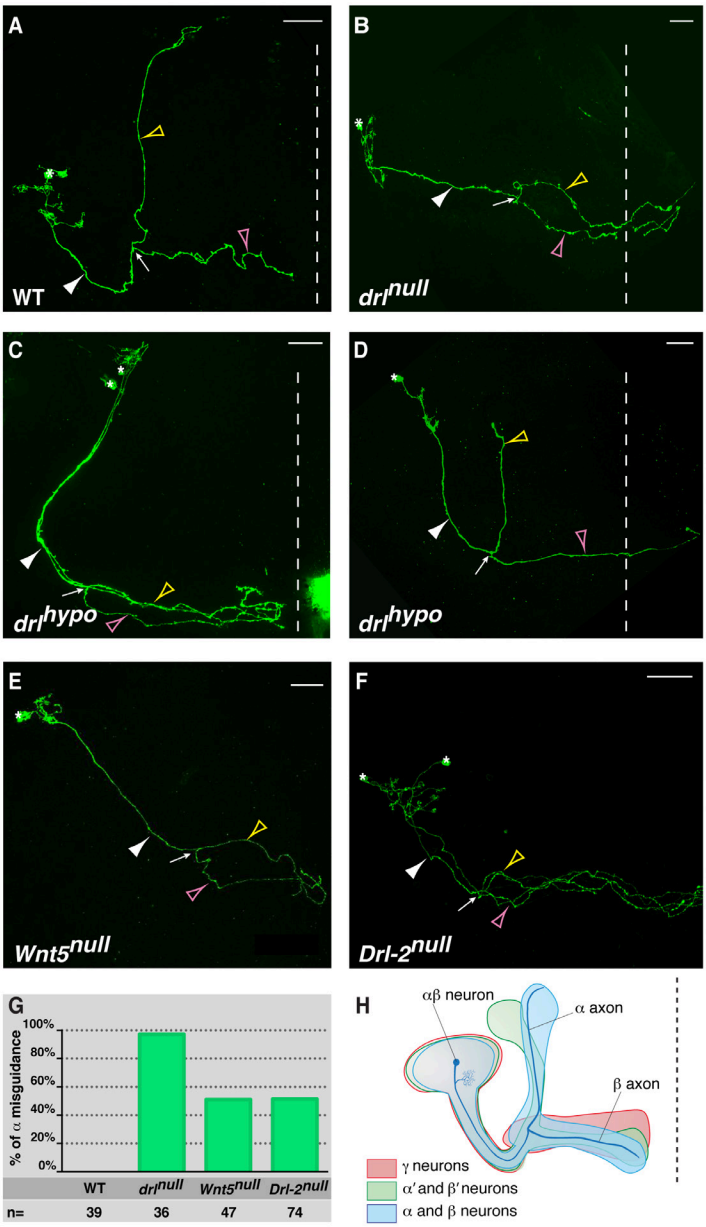

Figure 1. DRL, WNT5 and DRL-2 are required for MB α branch guidance (A) A single αβ neuron clone in a wild-type brain. (B) A single αβ neuron clone in a *drl*^{null} brain displaying α misguidance and inappropriate midline (dotted line) crossing of both the α (yellow arrowhead) and β (pink arrowhead) axons. (C and D) Neuron clones in *drl*^{hypo} individuals reveal the uncoupling of the α-misguidance and midline crossing phenotypes. (E and F) Neuron clones in *wnt5*^{null} (E) and *drl-2*^{null} (F) brains display α misguidance. In all images, the white arrow indicates the αβ branch point and the white arrowhead indicates the peduncle. (G) Quantitation of the penetrance of the α misguidance phenotype in the different mutant and control neuron clones. n=number of clones analyzed. See genotypes and other details in Supplemental Information for Figure 1. (H) Schematic representation of an αβ neuron in the context of the MB lobes. See also Figures S1, S2 and Tables S1, S2. 26

Table S2), indicating that WNT5 is involved in α axon branch guidance.

DRL is not detectably expressed within the MBs nor does *UAS-drl* expression driven by MB-specific GAL4 drivers rescue the *drl*^{null} phenotype (Grillenzoni et al., 2007). DRL, therefore, is unlikely to be an intrinsic α branch WNT5 receptor. To further rule out the possibility that DRL expression is required within the MBs, we used the *MB247-GAL80* (*MB-GAL80* (Krashes et al., 2007) transgene to suppress GAL4 activity in the MBs while expressing *drl* in all neurons with *elav-GAL4*. Expression of *MB-GAL80* suppressed the GAL4-driven pan-neural expression of a *mCD8-GFP* (*mGFP*) reporter to undetectable levels specifically only in the MBs both at 48 h APF and in the adult (data not shown) indicating its effectiveness. Pan-neural expression of *UAS-drl* in all non-MB neurons rescued the *drl*^{null} mutant MB phenotype to the same extent as when *drl* was expressed in all neurons (Figure 2A). Thus, DRL is required outside of, not within, the MB axons to ensure correct α branch guidance.

DRL-2 acts as an MB-intrinsic signaling receptor for α guidance

What is the intrinsic MB receptor that interacts with the WNT5 ligand to guide α axons? DRL-2 and DNT (doughnut) are the two other *Drosophila* Ryks (Fradkin et al., 2010) and therefore represented plausible candidates. Homozygous *dnt*^{null} mutants (Lahaye et al., 2012) did not display any MB phenotype (data not shown). Conversely, *drl-2*^{null} mutant neurons displayed α axon misguidance (Figure 1F). The analysis of *drl-2* mutant brains with *c739- GAL4* line (Figure S2) revealed absence of α lobe (circa 60% of the MBs) as well as wildtype MBs (circa 35%). Altogether, 51% (n=74) of the *drl-2*^{null} visualization MARCM clones displayed α misguidance (Figure 1G and Table S2). If we take into account only where α axons are affected, examination of visualization MARCM clones in *drl-2*^{null} brains revealed that α misguidance occurred in 90% of them (n=41) while the other 10% exhibited growth defects (Figure S2 and Table S2). Strikingly, *drl-2* acts non-cell-autonomously in *drl-2*$^{-/-}$ regular MARCM αβ MB neuroblast clones in otherwise *drl-2* heterozygous animals. These clones displayed wild type α guidance (data not shown). Similar non-cell-autonomous Wnt/Planar Cell Polarity-mediated MB axon branch extension defects were previously described for the membrane receptors *frizzled* and *strabismus* (Ng, 2012; Shimizu et al., 2011). Protein perdurance could be an alternative explanation of the absence of mutant phenotype displayed by *drl-2* regular MARCM clones. Nevertheless, two pieces of data strongly argue against the perdurance of DRL-2. First, the neuroblast clones are induced in L1, days before the birth of the αβ neurons. Second, the DRL-2 protein seems to be actively degraded (Figure S3). It is likely that mutant axons surrounded by wild type axons correctly pathfind by other mechanisms probably involving axon-axon interactions. Nevertheless, mutant rescue experiments with specific MB GAL4 lines led to the notion of MB-autonomy for these membrane receptors (Ng, 2012; Shimizu et al., 2011). Importantly, we were able to rescue *drl-2*^{null} α misguidance by expressing a *UAS-*

drl-2 transgene under the control of the MB αβ neuron-specific *c739-GAL4* driver (Aso et al., 2009) but not by expressing *drl-2* in all non-MB neurons or by inhibiting MB GAL4 expression from *c739-GAL4* by expression of GAL80 in the MB's (Figure 2B). Also, *201Y-GAL4* as well as *c305a-GAL4*, strongly expressed into the γ and α'β' neurons respectively (Aso et al., 2009) failed to rescue the *drl-2*^{null} α misguidance phenotype when associated with a *UAS-drl-2* transgene (data not shown). These results indicate that *drl-2* plays an MB-autonomous role in α branch guidance. This MB axon-specific rescue supports our conclusion that *drl-2* is an MB axon-intrinsic receptor involved in α guidance.

Does DRL-2 transduce an intracellular signal in the MB axons? We generated a *UAS-drl-2Δcyto* transgene and it failed to rescue the loss of the α lobe, indicating that DRL-2 likely transduces the WNT5 signal in MB axons (Figure 2B). Supporting our identification of DRL-2 as an MB-intrinsic WNT5 receptor, DRL-2 protein was detected in the growing α branch at 48 hours after puparium formation (APF) in wild type, but not in *drl-2*^{null} mutant, brains (Figure S3). No apparent difference in the levels of DRL-2 between the α and β branches were detected making it unlikely that DRL-2 localization determines why the b axon trajectories are unaffected in the *drl-2*^{null} mutant background. We then determined whether DRL-2 interacts with WNT5. Epitope-tagged DRL-2 bound WNT5, while DRL-2 lacking its Wnt-binding WIF domain did not, indicating that DRL-2 binds WNT5 via its WIF domain (Figure S4). Therefore, we performed further genetic experiments to determine whether *wnt5* interacts with *drl-2* to guide α axons.

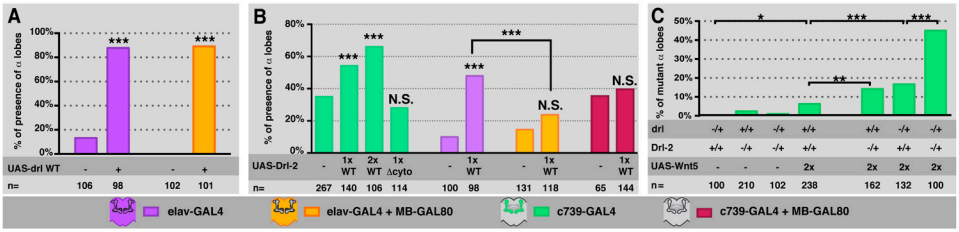

Figure 2. DRL and DRL-2 interact with WNT5 and are required to guide α branch axons (A) Rescue of the *drl*^{null} mutant phenotype by pan-neural expression of *UAS-drl WT* driven by *elav-GAL4* (purple) versus expression of *UAS-drl WT* in all non-MB neurons in the *elav-GAL4*; *MB-GAL80* background (orange). (B) Rescue of the *dl-2*^{null} mutant phenotype by *UAS-drl-2* but not by *UAS-drl-2Δcyto*, driven by the αβ specific *c739-GAL4* driver (green). Rescue of *drl-2*^{null} by *UAS-drl-2* driven in all neurons by *elav-GAL4* (purple) but not in all non-MB neurons by *elav-GAL4; MBGAL80* (orange). *c739 MB-GAL80* failed to rescue the *drl-2*^{null} MB phenotype when associated with a *UAS-drl-2* transgene by inhibiting MB GAL4 expression from *c739-GAL4* (red). (C) *drl*, *drl-2* and *wnt5* genetically interact during α branch guidance. For all panels, n=number of MBs analyzed, and ***: P <0.001, **: P <0.01, *:P <0.05, N.S.: not statistically different by χ^2 test. See genotypes and other information in Supplemental Information for Figure 2. See also Figures S3 and S4.

drl-2, *wnt5* and *drl* interact genetically during α branch guidance

Next we examined whether DRL-2 could act as an axon-repulsing WNT5 receptor in another context. Ectopic expression of wild-type *drl*, under control of the *eg-GAL4* driver, in *Drosophila* embryonic posterior commissure (PC) axons, which normally do not express DRL, causes them to cross in the adjacent anterior commissure due to their repulsion by WNT5 which is predominantly expressed by PC neurons (Bonkowsky et al., 1999). We found that expression of two copies of *UAS-drl-2* driven by *eg-GAL4* resulted in >95% axon commissure switching (Figure S4) in the wild type background. DRL-2-dependent switching was essentially completely suppressed by the absence of WNT5. Together, these results indicate that DRL-2 can act as a WNT5 axon-repulsing guidance receptor. We conclude that DRL-2 is likely an intrinsic MB receptor, which mediates a repulsive WNT5 signal required for α axon guidance.

Do *wnt5*, *drl-2* and *drl* genetically interact during α branch guidance? We were not able to detect genetic interactions even in the triple heterozygous condition ($wnt5^{+/-}$; $drl^{+/-}$ $drl\text{-}2^{+/-}$ 100% WT MBs, n = 102). Nevertheless, we noticed that when *wnt5* was strongly overexpressed in the MBs a modest but significant fraction (less than 10%) of the MBs showed α lobe misguidance (Figure 2C). The simplest interpretation for this phenotype could be that an excess of WNT5 emanating from the MBs is binding to DRL-2 receptor but does not provide a guidance cue because it is not bound and localized by extrinsic DRL (see below). Thus, the amount of available DRL-2 receptor would be decreased. In this situation, reducing the amount of DRL would further increase the amount of free WNT5 and reducing the dose of *drl-2* will further decrease the amount of available DRL-2. Indeed, when *drl* or *drl-2* is heterozygous ($drl^{+/+}$ or $drl\text{-}2^{+/+}$) in the WNT5 over-expressing background, α misguidance significantly increased relative to the controls (Figure 2C). Finally, we observed a dramatic increase in α misguidance in $drl^{+/+}$; $drl\text{-}2^{+/+}$ brains overexpressing WNT5 (Figure 2C), indicating that *drl*, *wnt5* and *drl-2* interact to guide α axons.

DRL is expressed by the lineages giving rise to the central complex and localizes WNT5

Where is DRL expression required to control α axon guidance? We tested a number of brain GAL4 drivers, which do not express in the MBs, for their ability to rescue the drl^{null} phenotype (data not shown). We identified *distalless (Dll)-GAL4* which is expressed in the dorsomedial (DM) lineages in the postembryonic brain (Izergina et al., 2009). DM neuroblast lineages contribute to the developing central complex but not the MB (Bayraktar et al., 2010; Izergina et al., 2009). Indeed, we did not observe *Dll-GAL4* expression in the developing MBs from the third larval instar to adult stages (data not shown and Figure S5) confirming previous reports. At the third larval instar stage, DRL is expressed in six large groups of cells at the DM margins of the brain hemispheres (Figure 3A). Upon double-labeling brains expressing

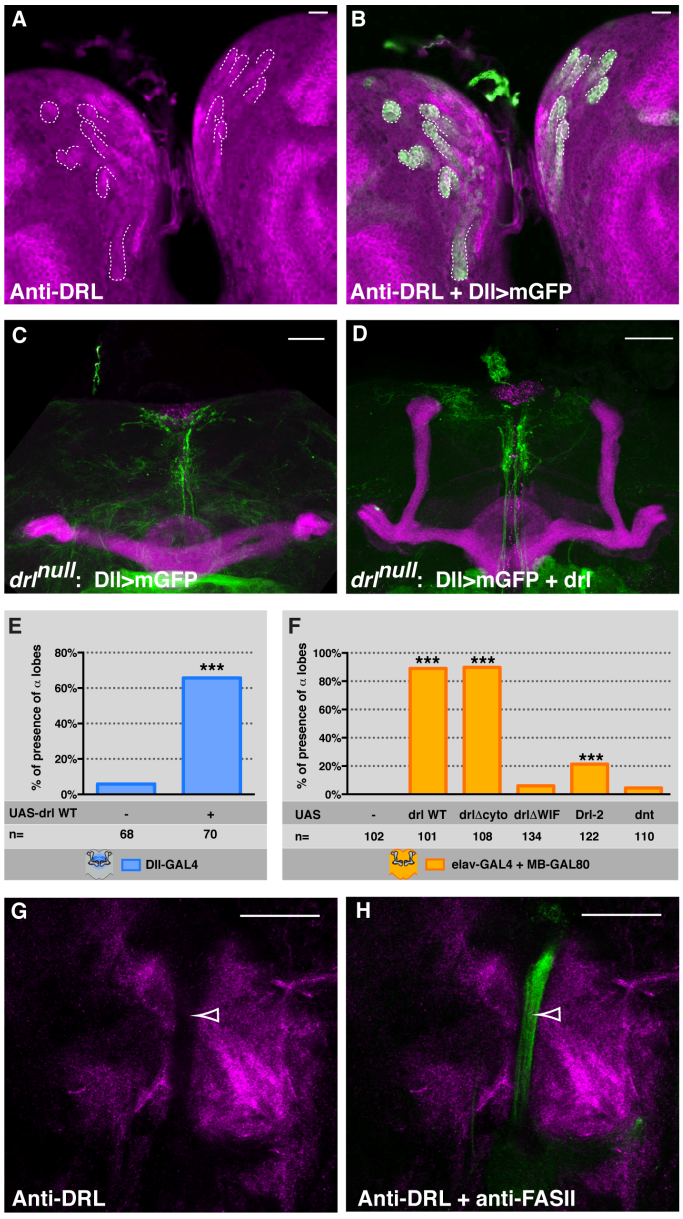

Figure 3. DRL is expressed in the dorsomedial lineages, precursors of the central complex (A) DRL (magenta) is expressed in six large groups of cells at the DM margins of the 3rd instar brain hemispheres (dotted outlines). (B) These cells are identified as DM lineage neurons by co-localization of DRL and GFP in brains expressing mGFP (green) driven by *Dll-GAL4*. (C and D) Anti-FASII staining (magenta) reveals the absence of the α lobes in a drl^{null} brain (C) which is rescued by expression of *UAS-drl WT* driven by *Dll-GAL4* (green; D). (E) Quantitation of α lobe rescue by *Dll-GAL4* (blue). (F) Quantitation of rescue of the drl^{null} phenotype by *drl WT, drl Δcyto* or *drl-2*, but not by *drl ΔWIF* or *dnt*. All constructs are driven by *elav-GAL4; MB-GAL80* (orange). n=number of MBs analyzed and ***: $P < 0.001$ (χ^2 test). (G and H) 24 hours APF WT brains. DRL (magenta) is expressed around, but not in (white arrowhead) the FASII positive α branch (green). See genotypes and details in Supplemental Information for Figure 3. See also Figure S5.

mGFP driven by *Dll-GAL4* with anti-GFP and anti-DRL, we observed colocalization of DRL and GFP in these cells (Figure 3B). Expression of DRL in the DM lineages rescued the *drl*^{null} phenotype (Figures 3C-3E). The spatial relationship between the *Dll-GAL4* neurons and the MBs was studied from 0 hours to 48 hours APF and revealed a close proximity of the *Dll-GAL* expressing neurons and the developing MBs (Figure S5). Expression of DRL lacking its cytoplasmic domain (*UAS-drlΔcyto*), but not DRL lacking its Wnt-binding WIF domain (*UAS-drlΔWIF*), in all non-MB neurons rescued the mutant phenotype to the same extent as the *UAS-drl WT* (Figure 3F). Therefore, although DRL must bind WNT5 to act, signaling through DRL is not required for α branch guidance. DRL's expression in the cells surrounding the MBs at 24 hours APF, but not in them (Figures 3G and 3H), is consistent with a MB-extrinsic role for DRL in α axon guidance. Does extrinsic DRL act to properly localize WNT5 to guide α axons? WNT5 is broadly expressed in the developing brain but a clear WNT5-free channel is present at the level of the α MB lobes (Shimizu et al., 2011). We found that WNT5 was mis-expressed in this region in *drl*^{null} brains as early as 24 hour APF (Figure 4). This result indicates that WNT5 distribution in the brain is controlled, at least in part, by the DRL receptor. WNT5 expression appeared globally increased in the *drl* mutant brain. Indeed, *wnt5* transcript levels, quantitated by qRT-PCR of 3rd instar brain RNA, were increased 1.5-fold in *drl* mutant brains, relative to controls (data not shown). Therefore in the developing brain, DRL acts to regulate *wnt5* mRNA levels in addition to its role in localizing the WNT5 protein.

Cleavage and release of DRL's ectodomain is required for α branch guidance

DRL's extracellular domain (ECD) was detected at 48 hours APF on the tips of the MB lobes (Figures 5A-5F). Interestingly, DRL was found at significantly higher levels at the α lobe tip than at the β lobe tip (Figure 5G). This is the only clear molecular difference between the α and the β lobes thus far reported and might be relevant to the *drl* mutant phenotype when only the α trajectory is affected. Importantly, the intracellular domain of DRL tagged by a C-terminal MYC epitope tag was not found at the tip of the wild-type α lobe when a *UAS-drl-WT-MYC* transgene was overexpressed in the DM lineages (Figure 6), indicating that the cytoplasmic domain of DRL is not localized to the α lobe tip. Thus we conclude that the DRL species present at the α lobe tip consists of only the Wnt-binding ECD.

Since *drl* expression is not required in the MBs, yet the DRL ECD was localized to the MB lobe tips, we tested the hypothesis that DRL's ECD is released by proteolysis and shed from expressing cells to guide α axons. DRL has a putative tetrabasic cleavage (TBC) site whose cleavage would result in the extracellular shedding of DRL's ECD bearing the intact Wnt-binding domain. We mutated the TBC site (KRKK>AAAA) to generate a *UAS-drlΔTBC* transgene. Although one copy of wild-type transgene strongly rescued, even two copies of the *UAS-drlΔTBC* transgene failed to rescue the *drl*^{null} α lobe misguidance phenotype (Figure

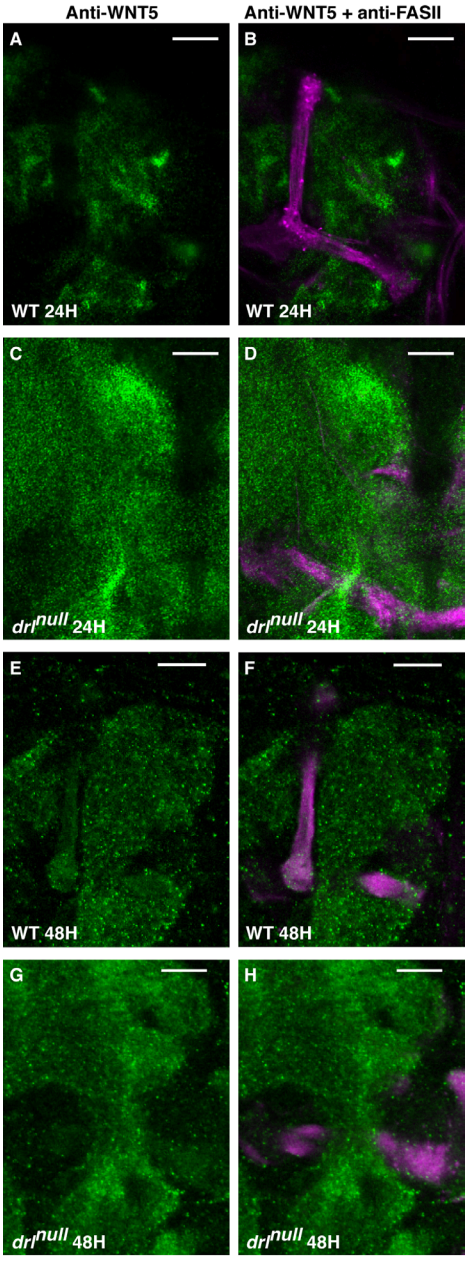

Figure 4. DRL restricts WNT5 expression in the brain (A, B, E, and F) Wild-type 24 h APF (A and B) and 48 h APF brains (e,f) stained with anti-WNT5 (green) and anti-FASII (magenta) revealed a WNT5-free channel at the level of the α 28 MB lobes. At 48 h APF WNT5 is expressed within the MB lobes but the channel was still apparent. (C, D, G, and H) *drl*^{null} 24 h APF (C and D) and 48 h APF brains (G and H) where WNT5 was mis-expressed in the channel region. The confocal laser and acquisition and processing settings were the same for the wild-type and mutant. At 24 h APF, 6 MBs were analyzed in both cases (WT and *drl*^{null}) with 0 mutant and 6 wildtype MBs for WT and 4 mutant and 2 wild-type for *drl*$^{null.}$ At 48 h APF, 6 MBs were analyzed for WT and 12 MBs for *drl*^{null} with 0 mutant and 6 wild-type MBs for WT and 10 mutant and 2 wild-type for *drl*$^{null.}$ Genotypes: (WT) *w* ^{1118}/*y w*^{67c23} (24 h APF), *w* ^{1118} (48 h APF). (*drl*^{null}) *w* ^{1118} /*w*^{1118} ; *lio*^{2} /*drl*^{R343}. Scale bars represent 20 μm. Images are single confocal sections.

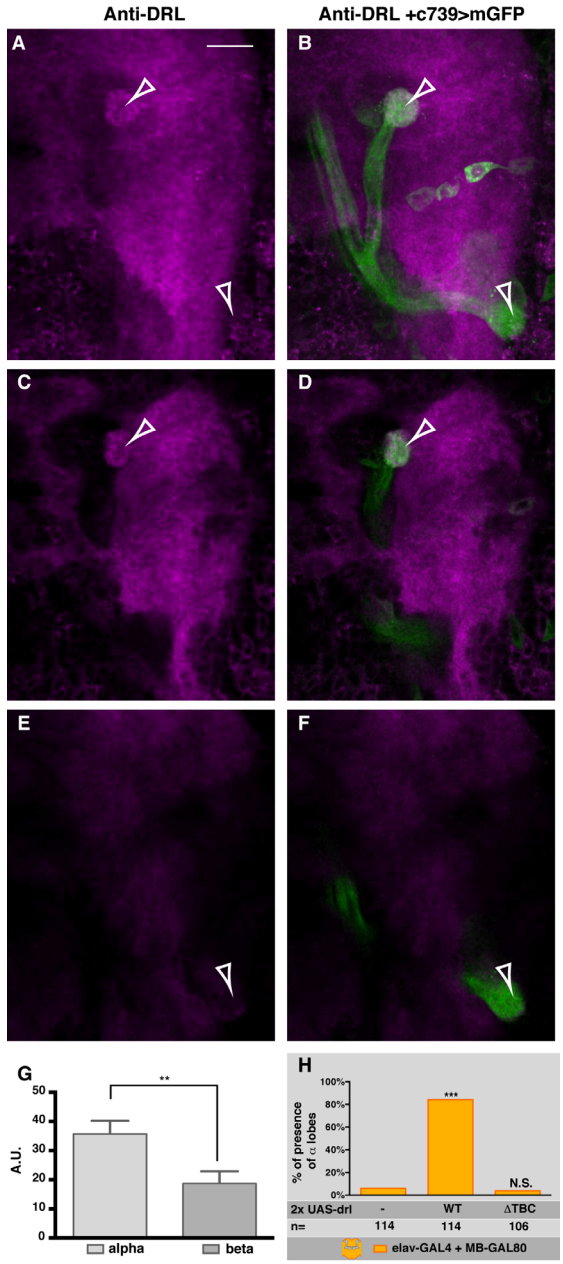

Figure 5. DRL is present at the tips of the MB lobes and DRL's TBC site is required to rescue the mutant phenotype (A-F) *c739-GAL4 UAS-mCD8GFP* 48 h APF brain. DRL (magenta), detected with an antibody recognizing the ECD, is present at the tip (arrowheads) of the MB lobes (GFP in green). (A and B) 40 confocal sections. (C-F) 1 confocal section. (G) Quantitation of the intensity of the DRL signal, normalized to that of GFP, in arbitrary units (A.U.). Results are means +/- SEM. n=5 MBs analyzed. DRL was present significantly more at the α lobe tip than at the β lobe tip. **: $P < 0.01$ (paired t test). (H) DRL's TBC site is required for MB-extrinsic guidance of the α lobe. n=number of MBs analyzed, and ***: $P < 0.001$, NS: not statistically different (χ^2 test). See genotypes and details in Supplemental Information for Figure 5.

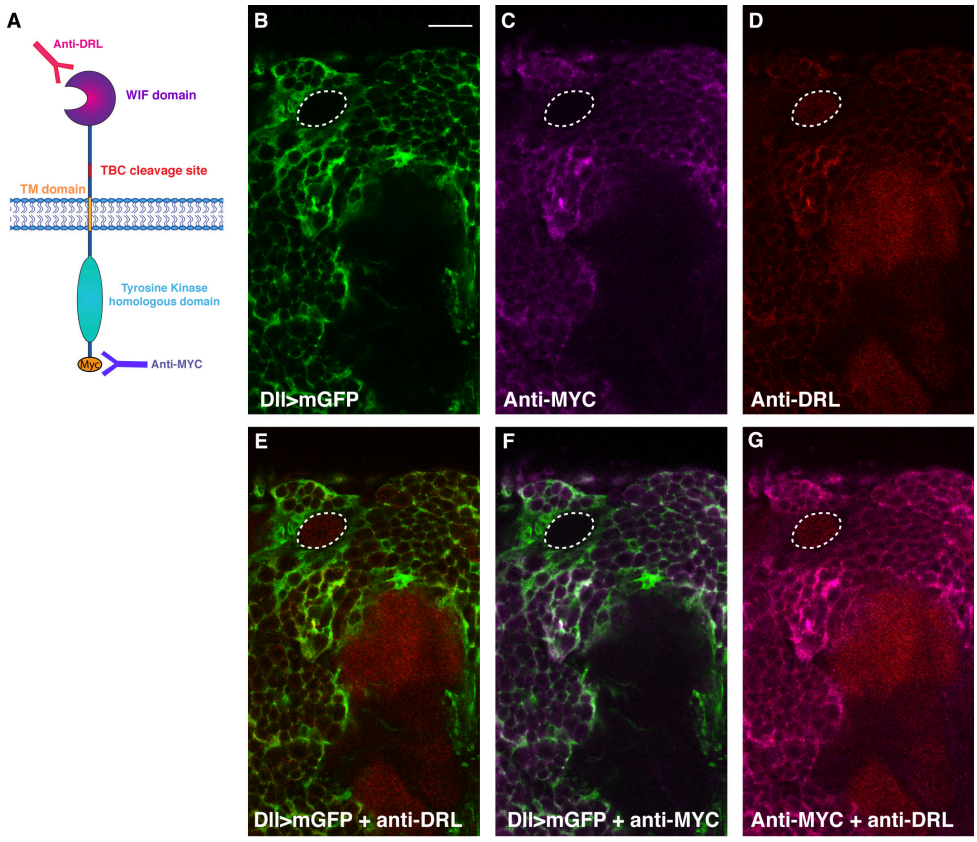

Figure 6. The cleaved DRL ECD is present at the tip of the MB α lobe (A) Schematic representation of the DRL ECD and intracellular domain recognized respectively by the anti-DRL and by the anti-MYC antibody. (B-G) All images shown are of 48 h APF *UAS-mCD8GFP Dll-GAL4* brains. Green represents *Dll-GAL4* driven GFP, red indicates anti-DRL and magenta anti-MYC. The DRL ECD, revealed by the anti-DRL antibody (red), was found at the tip of the MB α lobe (dotted circle in D, E, and G). The intracellular domain of DRL tagged by a carboxyterminal MYC epitope tag (magenta) was not found at the tip of the α lobe when a *UAS-drl-WT-MYC* transgene was overexpressed under *Dll-GAL4* driver control (dotted circle in C and F). Thus, we conclude that the DRL species present at the α lobe tip consists of only the Wnt-binding ECD. Genotype: *UAS-drl WT-MYC/y w* $^{67c23;}$ *UAS-mCD8GFP Dll-GAL4 /+*. Scale bars represent 20 µm. Images are single confocal sections. See also Figures S6 and S7.

5H and Figure S6 for the sub-cellular specificity of *UAS-drlΔTBC* transgene expression). We also observed that DRL ECD displayed limited diffusion throughout the brain when the TBC site was mutated (Figure S7) further supporting the hypothesis that DRL's ECD is released by cleavage at the TBC site. Finally, anti-MYC immunoblot analyses of 3rd instar brains expressing either DRL-WT-MYC or DRL-ΔDTBC-MYC revealed the presence of a MYC-tagged species corresponding in size to the expected intracellular cleavage product only from animals expressing wild type DRL (Figure S7I). This further reinforces the likelihood that DRL is cleaved at the TBC site *in vivo*.

The DRL ECD forms a WNT5-dependent complex with DRL-2

WNT5 is enriched at the tips of the lobes, in the 48 hours APF MBs (Shimizu et al., 2011) (and data not shown). The presence of both WNT5 and DRL's ECD at the tips of the 48 hours APF α lobes raised the question as to whether the DRL's ECD might form a ternary complex with WNT5 and the MB-intrinsic DRL-2. To investigate this possibility, we transfected Schneider S2 cells with DRL-2 and WNT5 expression constructs. After 48 hours, cells were harvested, washed and resuspended in serum-free media in the presence of soluble Fc-DRL-ECD, to mimic the DRL ECD species liberated by cleavage at the TBC site, or control human IgG. Fc-containing complexes were captured on Protein A agarose, washed and then subjected to SDS-PAGE and immunoblotting for DRL-2. We found that the Fc-DRL-ECD precipitated DRL-2 only when WNT5 was also expressed (Figure 7). We conclude that DRL's ECD interacts with DRL-2 in a WNT5-dependent manner.

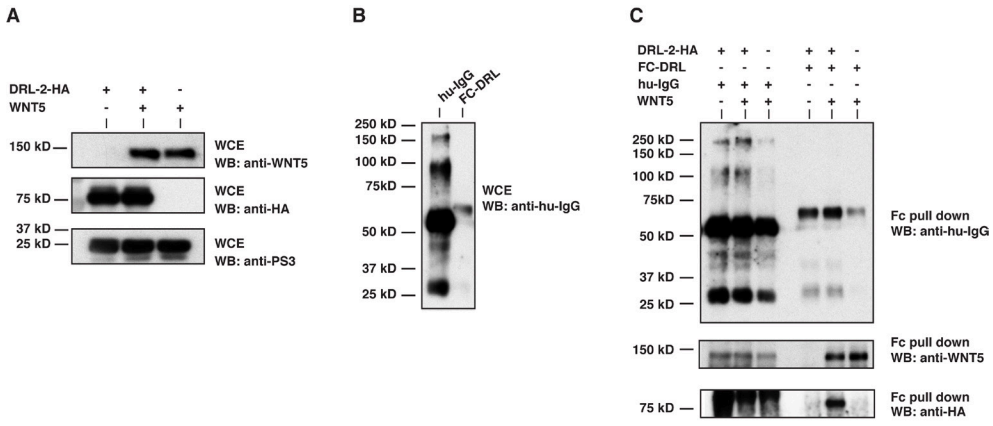

Figure 7. The DRL ECD forms a WNT5-dependent complex with transmembrane DRL-2 (A) Immunoblots of whole cell extracts (WCE). (B and C) Immunoblots of the Fc immunoprecipitations. S2 cells were transfected with the indicated expression constructs. 48 hours post-transfection, cells were washed and transferred to serum-free media containing either Fc-DRL ECD or control human IgG. Fc-containing complexes were captured on Protein A beads, washed and proteins analyzed by SDS-PAGE and immunoblot with anti-WNT5 and anti-HA antibodies to detect co-immunoprecipitating WNT5 and DRL-2, respectively. DRL-2 precipitated with the DRL ECD only in the presence of WNT5 indicating that these proteins form a ternary complex. The bands in the human IgG immunoprecipitations on the lower two blots are nonspecific as evidenced by their presence in all three samples. The data shown are representative of three experiments.

DISCUSSION

Here, we have shown that the wild-type guidance of the MB α axons results from an interplay between two *Drosophila* Ryks. DRL, expressed outside of, but near the MBs, interacts with DRL-2, which is expressed on MB axons, via their common ligand, WNT5. These interactions between DRL, WNT5 and DRL-2 during α axon guidance contrast with those described for the patterning of the antennal lobes (ALs). DRL in the ALs likely sequesters WNT5 and prevents it from signaling through DRL-2 (Sakurai et al., 2009; Yao et al., 2007). Loss-of-function alleles of all three genes display MB α axon misguidance indicating that these proteins, in contrast to their roles in the ALs, act together, rather than antagonistically, to guide α axons. Strikingly, while the β axon trajectories are unaffected in the *drl* and *drl-2* mutants, these axons often fail to stop at the midline indicating roles for DRL and DRL-2 in the cessation of β axon extension. Further studies will be required to understand the control of β axon extension and to identify the other mechanisms that guide them medially.

We suggest that the DM lineage DRL expression domain in the pupal brain surrounds the growing α MB lobe where transmembrane DRL captures WNT5 and limits its diffusion. Supporting this is our observation that WNT5 invades this region in the absence of DRL. DRL-bound WNT5 repulses the extending DRL-2-expressing α axon growth cones, preventing their medial migration, thus causing them to navigate dorsally. Our observation that DRL's TBC site is required for α axon guidance indicates a likely need for DRL's ECD to be shed to effect α axon guidance. We cannot visualize the DRL ECD/WNT5 complex on single growing neurons but the presence of DRL ECD and WNT5 at the tips of the α branch axons at 48 hours APF of MB development likely reflects the history of the α axon growth cone interaction with the DRL ECD/WNT5 complex. The continued presence of this complex at the a lobe tip raises the interesting question as to whether this complex stably modulates DRL-2 signaling. Resolving this question will require the identification of MB signaling pathway members downstream of DRL-2.

The role of axon guidance receptor guiding axons in which it is not expressed is not unprecedented. In *Drosophila*, the *frazzled* (*fra*) receptor guides specific embryonic central nervous system axons and lamina layer-specific targeting of photoreceptor axons by controlling the distribution of its ligand, Netrin (Hiramoto et al., 2000; Timofeev et al., 2012). The embryonic axons apparently employ an unidentified intrinsic receptor which is not FRA (Hiramoto et al., 2000) while the Netrin receptor expressed by the incoming photoreceptor is FRA itself (Timofeev et al., 2012). Unlike DRL, FRA at the lamina target site requires its cytoplasmic domain for its own proper localization and function in localizing Netrin (Hiramoto et al., 2000). No evidence that FRA needs to be proteolytically-processed for its roles in either

tissue has been presented. Strikingly, a recent report of the structure of Netrin complexed with two of its receptors revealed that Netrin has two distinct receptor binding sites (Xu et al., 2014). Wnt protein binding has been shown to oligomerize the Frizzled and LRP co-receptors expressed on the same cell surface likely by binding to both receptors (Cong et al., 2004). Existing biochemical and structural data, however, do not explicitly address whether monomeric Wnt proteins can simultaneously bind to two receptors as does Netrin or whether Wnts act in complexes containing multiple Wnt proteins such as aggregates or by being displayed on the surface of exosomes (Beckett et al., 2013; Gross et al., 2012). Nonetheless, such a ligand-dependent *trans*-interaction between two Wnt receptors on different cells, as we have shown here for DRL and DRL-2 has not been previously reported to our knowledge.

The regulation of axon guidance receptors by proteolytic processing has also been documented for several axon guidance molecules, although in most cases only *in vitro* data are available (reviewed in (Bashaw and Klein, 2010)). Extracellular domains of transmembrane proteins, including cell surface signaling receptors, are often shed by regulated intramembrane proteolysis (reviewed in (Brown et al., 2000)) to effect extracellular roles or simply as a byproduct of a requirement to release the intracellular domain. In most cases proteolytic processing triggers cytoplasmic signaling pathways. The interaction of membrane-bound Ephrin ligand with the Eph receptor (Hattori et al., 2000) provides an example of the role of a ligand-bound extracellular domain superficially similar to that of WNT5/DRL ECD. Regulated proteolytic cleavage of the membrane-bound ligand enhances growth cone retraction. A more recent study of the role of EphA4 receptor cleavage during spinal motor neuron guidance demonstrated that EphA4 cleavage in the mesenchymal target is required to allow the target-derived ephrinA ligand to interact with EphA4 present on the axon (Gatto et al., 2014). Cleavage-resistant EphA4 sequesters target-derived ephrinA preventing it from repulsing the axon. In contrast, our data support a model where WNT5-binding and cleavage of the DRL ECD is required to facilitate WNT5 signaling through DRL-2. Another clear difference between Eph and DRL mechanisms is that, unlike ephrin, WNT5 is a secreted non-membrane bound protein. Finally, although the individual steps, ligand-localization and ectodomain shedding, that we have demonstrated to be necessary for DRL's role in a axon guidance have precedents, to our knowledge this combination of steps has not been previously reported for an axon guidance receptor.

The DRL ECD may act similarly to the secreted Wnt-binding signaling modulators such as the sFRPs (secreted Frizzled-related proteins) and Dickkopf proteins (reviewed in (Cruciat and Niehrs, 2013)). However, the difference between WNT5 bound to membrane-anchored DRL versus to a secreted Wnt-modulatory protein is the specificity of their spatial localization. DRL-bound WNT5 could provide a localized repulsive cue to guide axons, while it is unlikely

that a widely-expressed freely-diffusing secreted protein could provide a directional signal. Is this axon guidance mechanism conserved? *Drosophila* expresses three Ryks, however, all other higher eukaryotes express only one. Our finding that *drl* can rescue the *drl-2* mutant phenotype when expressed in MB neurons (data not shown) indicates that a single Ryk expressed in axons and structures adjacent to them would suffice to guide them. This is further supported by the invariant conservation of the TBC site in all Ryks. Strikingly, DRL's TBC site is also required for its role during embryonic pathfinding (Petrova et al., 2013) where its cytoplasmic domain, and hence likely signal transduction, is required (Petrova et al., 2013; Yoshikawa et al., 2001). This indicates that cleavage at the juxtamembrane site, likely in addition to an intramembrane cleavage, is possibly necessary for receptor endocytosis or freeing the intracellular domain for transport to the nucleus, the latter having been reported for mammalian Ryk (Lyu et al., 2008).

In both the *Drosophila* embryonic nerve cord and in the developing MBs, localized WNT5 acts as a Ryk guidance cue. WNT5 localization is, however, achieved by two different mechanisms. During embryogenesis, WNT5 is preferentially expressed by posterior commissural neurons since DRL represses *wnt5* transcription in anterior commissural neurons (Fradkin et al., 2004). In the MBs, we have shown that WNT5 is localized in a para-MB pattern via the interaction of WNT5 with extrinsic DRL. We also demonstrated that the DRL ECD is shed and forms a ternary complex with WNT5 and the axon-intrinsic DRL-2 receptor. The capture and localization of a widely-expressed ligand to the surfaces of cells nearby axons to guide those axons as well as the formation of a ternary complex by a shed ECD, the ligand and an axon-intrinsic receptor may likely prove to be conserved developmental strategies.

EXPERIMENTAL PROCEDURES

Drosophila stocks

All crosses were maintained on standard culture medium at 25°C. The following alleles were used, *lio2* , drl^{R343} , $wnt5^{400}$ and $drl\text{-}2^{E124}$. Except where otherwise stated, all alleles have been described previously (http://flystocks.bio.indiana.edu/). To examine the effects of homozygosity for drl^{null} and for $drl\text{-}2^{null}$, we generated lio^{2} /drl^{R343} and $drl\text{-}2^{E124}$/Df(2R)Exel8057 animals, respectively, to minimize the effects of the genetic backgrounds of homozygosity for the individual alleles.

Brain dissection, MARCM mosaic analysis and visualization

Pupal brain dissection and immunostaining

Brains were dissected and treated as previously described (Timofeev et al., 2012). They were incubated in PBS with 0.5% Triton X-100 (PBT) and 5% normal horse serum (blocking solution) at room temperature for 30 minutes, followed by overnight incubation at 4°C with

primary antibodies diluted in blocking solution. Brains were then washed three times in PBT for 20 min, followed by 30 min in the blocking solution, and then addition of the secondary antibodies with incubation for 2 h at room temperature. Brains were then washed in PBT for 2 h and were mounted with Vectashield (Vector Laboratories). Rabbit anti-DRL, guinea pig anti-DRL-2, mouse anti-MYC and rabbit anti-WNT5 were pre-absorbed with 10 *y w 67c23* heads and thoraxes in the blocking solution at the final dilution (1:2000, 1:1000, 1:1000 and 1:150, respectively). The pre-absorbed anti-DRL-2 was also pre-absorbed a second time using *drl-2*^{null} mutant 48 h APF brains. The following secondary antibodies were used at a dilution of 1:500: anti-rabbit Cy3 (Jackson ImmunoResearch) and anti-guinea pig Cy3 (Jackson ImmunoResearch). Anti-Fasciclin II (mAb 1D4 from DSHB) was used at 1:50 dilution followed by anti-mouse Cy3 (Jackson ImmunoResearch) at a dilution of 1:300. For 24 h and 48 h APF anti-WNT5 immunostaining, dissected brains were incubated with anti-WNT5 (1:150) in PBS at 4°C for 2 h 30 min, washed in 1x PBS and fixed in PLP for 1 h at room temperature, then the protocol above was followed.

Adult brain dissection and immunostaining

Fly heads and thoraxes were fixed for 1 h in 3.7% formaldehyde in PBS. Brains were dissected in PBS. They were then treated for immunostaining as previously described (Boulanger et al., 2011; Lee and Luo, 1999). Primary antibody used was anti-Fasciclin II (mAb 1D4 from DSHB) at 1:50 dilution followed by anti-mouse Cy3 (Jackson ImmunoResearch) at 1:300.

Presence of α lobes

An α lobe was considered as present when either an apparently complete wild-type lobe (more than 80% of the cases) or thinner lobe (less than 20% of the cases) with an estimated width ≥ 40% of that of wild-type lobe width, was seen using the FIJI software.

MARCM Clonal analysis

To generate clones in the MB, we used the Mosaic Analysis with a Repressible Cell Marker (MARCM) technique (Lee and Luo, 1999). For single- and two-cell clones, 48 h APF pupae were heat-shocked at 37°C for 15 min. For neuroblast clones, first instar were heat shock at 37°C for 1 h. Adult brains were fixed for 15 min in 3,7% formaldehyde in PBS before dissection and staining. We used the term “visualization MARCM clones” when homozygous mutant clones were examined in a homozygous mutant background and “regular MARCM clones” when homozygous mutant clones were examined in a heterozygous background.

Axon commissure switching assay

The assay was performed essentially as described previously (Callahan et al., 1995) except *UAS-mCD8-GFP* was included to allow visualization of the *eg*$^{+}$ axons by staining with anti-GFP (Roche) and anti-CD8 (Life Sciences)

Quantitative qRT-PCR

RNA from 3rd instar brains was prepared using RNAeasy (Qiagen) according to the manufacturer's specifications and reversed transcribed using the IScript cDNA Synthesis Kit (Biorad). cDNA was amplified on a CFX384 Real Time PCR System (BioRad) using Power SYBR Green PCR Master Mix (Applied Biosystems) and intron-spanning primers hybridizing to the *wnt5* gene and *RP49* control. *wnt5* RNA levels are reported in arbitrary units normalized to *RP49* levels

Microscopy and image processing

Images were acquired at room temperature using a Zeiss LSM 780 laser scanning confocal microscope (MRI Platform, Institute of Human Genetics, Montpellier, France) equipped with a 40x PLAN apochromatic 1.3 oil-immersion differential interference contrast objective lens. The immersion oil used was Immersol 518F. The acquisition software used was Zen 2011. Contrast and relative intensities of the green (GFP) and magenta (Cy3) channels were processed with Imaris and FIJI software. The angles between α and β axon branches were measured using the angle tool of FIJI software.

Constructs, transgenic flies, transfections, immunoprecipitation and immunoblotting

HA-tagged actin promoter-driven wild-type *drl-2* and *drl-2* lacking its WIF domain (*ΔWIF*) and MYC-tagged UAS wild-type *drl* and *drl-2* and their mutants lacking the cytoplasmic or WIF domain expression plasmids were constructed by ORF PCR, oligonucleotide-mediated mutagenesis and Gateway-mediated recombination (Invitrogen) into appropriate destination vectors (provided by T. Murphey; http://www.ciwemb.edu/ labs/murphy/ Gateway%20 vectors.html). Fc-DRL ECD was constructed by appending DRL ECD-coding sequences in frame to the FC ORF (kindly provided by John Thomas) and the fusion protein ORF was subsequently transferred into the pDEST10 baculovirus vector. Recombinant Fc-DRL ECD expressing baculovirus were generated using the Bac-to-Bac system (Invitrogen) and FcDRL-ECD protein was purified by Protein A chromatography from infected Sf9 cell culture supernatants. All constructs were verified by DNA sequencing. S2 cell transfections were performed using Effectene (Qiagen). MYC-tagged *drl-* and *drl-2* expressing transgenic fly lines (UASs) were generated by BestGene and MYC expression-matched lines (DRL species) and transgenes inserted into the same *attP* site (DRL-2) were subsequently used. Western blot analyses indicate that the *UAS-drl* (WT, Δcyto and ΔWIF) species are similarly expressed when driven by *elav-GAL4* in the 3rd instar larval brain. Lysates were prepared using a high-stringency buffer (50mM Tris-HCl, pH 8.0; 150 mM sodium chloride ; 1% NP40; 0.5% sodium deoxycholate; 0.1% SDS; 0.2 mM sodium orthovanadate 10 mM sodium fluoride; 5 mM sodium pyrophosphate; 0.4 mM EDTA; 10% glycerol) containing protease inhibitors (Roche). For the immunoblot presented in Figure S7, lysates were prepared from

10 L3 brains homogenized in 1X NuPAGE LDS sample buffer (Invitrogen) containing 0.5 M DTT. Immunoprecipitations were performed using rabbit anti-HA (AbCam) and mouse anti-human Fc (Jackson Immunoresearch). Immunoblots, prepared by standard procedures, were incubated with mouse anti-HA (Sigma), rabbit anti-WNT5 (Fradkin et al., 2004) and mouse anti-MYC (DSHB). Anti–*Drosophila* ribosomal protein P3 (Kelley et al., 2000), kindly provided by M. Kelley and anti-mouse a-TUBULIN (Sigma) were used to control for equivalent gel loading. Bound multiple-label grade HRP-conjugated secondary antibodies (Jackson ImmunoResearch) were detected with enhanced ECL reagent (GE Healthcare).

Statistics

Comparison between groups expressing a qualitative variable was analyzed for statistical significance using the $\chi 2$ test. Comparison of two groups expressing a quantitative variable was analyzed using the two-tailed Student's t test. Comparison of the distribution of the ratios was analyzed using the Wilcoxon rank sum test. Values of $P < 0.05$ were considered to be significant.

Supplemental Information

Supplemental Information includes Supplemental Information for Figure 1-3 and 5, seven figures and two tables.

ACKNOWLEDGEMENTS

We thank Florence Besse, Alain Chédotal and Claude Desplan for thoughtful discussions and support, B. Bello for informing us that *drl* is expressed in the DM lineages and for the *Dll-GAL4* line, C. Hama for the *UAS-drl2* line and the anti-DRL-2 antibody, H. Korswagen, H. Hing for comments on the manuscript, the Bloomington *Drosophila* Stock Center for fly stocks and the MRI platform for confocal imaging help. Work in the laboratory of J-MD was supported by the Centre National de la Recherche Scientifique, the Association pour la Recherche sur le Cancer (n°3744 and SFI20121205950) and the Agence Nationale de la Recherche (ANR-07-NEURO-034-01). ER was supported by a Ph.D. grants from the Ministère de l'Enseignement Supérieur et de la Recherche and the Association pour la Recherche sur le Cancer. Work in the laboratory of JNN and LGF, with excellent technical help from Anja de Jong, was funded by the "Nederlandse Organisatie voor Wetenschappelijk Onderzoek" (N.W.O; ZonMw TOP Grant 40-00812-98-10058) and the Hersenstichting Nederland (HS 2013(1)-161).

REFERENCES

Aso, Y., Grubel, K., Busch, S., Friedrich, A.B., Siwanowicz, I., and Tanimoto, H. (2009). The mushroom body of adult *Drosophila* characterized by GAL4 drivers. J Neurogenet 23, 156- 172.

Bashaw, G.J., and Klein, R. (2010). Signaling from axon guidance receptors. Cold Spring Harb Perspect Biol 2, a001941.

Bayraktar, O.A., Boone, J.Q., Drummond, M.L., and Doe, C.Q. (2010). *Drosophila* type II neuroblast lineages keep Prospero levels low to generate large clones that contribute to the adult brain central complex. Neural Dev 5, 26.

Beckett, K., Monier, S., Palmer, L., Alexandre, C., Green, H., Bonneil, E., Raposo, G., Thibault, P., Le Borgne, R., and Vincent, J.P. (2013). *Drosophila* S2 cells secrete wingless on exosome-like vesicles but the wingless gradient forms independently of exosomes. Traffic 14, 82-96.

Bonkowsky, J.L., Yoshikawa, S., O'Keefe, D.D., Scully, A.L., and Thomas, J.B. (1999). Axon routing across the midline controlled by the *Drosophila* Derailed receptor. Nature 402, 540-544.

Boulanger, A., Clouet-Redt, C., Farge, M., Flandre, A., Guignard, T., Fernando, C., Juge, F., and Dura, J.M. (2011). ftz-f1 and Hr39 opposing roles on EcR expression during *Drosophila* mushroom body neuron remodeling. Nat Neurosci 14, 37-44.

Boyle, M., Nighorn, A., and Thomas, J.B. (2006). *Drosophila* Eph receptor guides specific axon branches of mushroom body neurons. Development 133, 1845-1854.

Brown, M.S., Ye, J., Rawson, R.B., and Goldstein, J.L. (2000). Regulated intramembrane proteolysis: a control mechanism conserved from bacteria to humans. Cell 100, 391-398.

Callahan, C.A., Muralidhar, M.G., Lundgren, S.E., Scully, A.L., and Thomas, J.B. (1995). Control of neuronal pathway selection by a *Drosophila* receptor protein-tyrosine kinase family member. Nature 376, 171-174.

Cong, F., Schweizer, L., and Varmus, H. (2004). Wnt signals across the plasma membrane to activate the beta-catenin pathway by forming oligomers containing its receptors, Frizzled and LRP. Development 131, 5103-5115.

Cruciat, C.M., and Niehrs, C. (2013). Secreted and transmembrane wnt inhibitors and activators. Cold Spring Harb Perspect Biol 5, a015081.

Dura, J.M., Preat, T., and Tully, T. (1993). Identification of linotte, a new gene affecting learning and memory in *Drosophila* melanogaster. J Neurogenet 9, 1-14.

Fradkin, L.G., Dura, J.M., and Noordermeer, J.N. (2010). Ryks: new partners for Wnts in the developing and regenerating nervous system. Trends Neurosci 33, 84-92.

Fradkin, L.G., van Schie, M., Wouda, R.R., de Jong, A., Kamphorst, J.T., RadjkoemarBansraj, M., and Noordermeer, J.N. (2004). The *Drosophila* Wnt5 protein mediates selective axon fasciculation in the embryonic central nervous system. Dev Biol 272, 362-375.

Gatto, G., Morales, D., Kania, A., and Klein, R. (2014). EphA4 receptor shedding regulates spinal motor axon guidance. Curr. Biol. 24, 2355-2365.

Grillenzoni, N., Flandre, A., Lasbleiz, C., and Dura, J.M. (2007). Respective roles of the DRL receptor and its ligand WNT5 in *Drosophila* mushroom body development. Development 134, 3089-3097.

Gross, J.C., Chaudhary, V., Bartscherer, K., and Boutros, M. (2012). Active Wnt proteins are secreted on exosomes. Nat Cell Biol 14, 1036-1045.

Hattori, M., Osterfield, M., and Flanagan, J.G. (2000). Regulated cleavage of a contactmediated axon repellent. Science 289, 1360-1365. Heisenberg, M. (2003). Mushroom body memoir: from maps to models. Nat Rev Neurosci 4, 266-275.

Hiramoto, M., Hiromi, Y., Giniger, E., and Hotta, Y. (2000). The *Drosophila* Netrin receptor Frazzled guides axons by controlling Netrin distribution. Nature 406, 886-889.

Izergina, N., Balmer, J., Bello, B., and Reichert, H. (2009). Postembryonic development of transit amplifying neuroblast lineages in the *Drosophila* brain. Neural Dev 4, 44.

Kelley, M.R., Xu, Y., Wilson, D.M., 3rd, and Deutsch, W.A. (2000). Genomic structure and characterization of the *Drosophila* S3 ribosomal/DNA repair gene and mutant alleles. DNA Cell Biol 19, 149-156.

Krashes, M.J., Keene, A.C., Leung, B., Armstrong, J.D., and Waddell, S. (2007). Sequential use of mushroom body neuron subsets during *drosophila* odor memory processing. Neuron 53, 103-115.

Lahaye, L.L., Wouda, R.R., de Jong, A.W., Fradkin, L.G., and Noordermeer, J.N. (2012). WNT5 interacts with the Ryk receptors doughnut and derailed to mediate muscle attachment site selection in *Drosophila* melanogaster. PLoS One 7, e32297.

Lee, T., Lee, A., and Luo, L. (1999). Development of the *Drosophila* mushroom bodies: sequential generation of three distinct types of neurons from a neuroblast. Development 126, 4065-4076.

Lee, T., and Luo, L. (1999). Mosaic analysis with a repressible cell marker for studies of gene function in neuronal morphogenesis. Neuron 22, 451-461.

Lyu, J., Yamamoto, V., and Lu, W. (2008). Cleavage of the Wnt receptor Ryk regulates neuronal differentiation during cortical neurogenesis. Dev Cell 15, 773-780.

Ng, J. (2012). Wnt/PCP proteins regulate stereotyped axon branch extension in *Drosophila*. Development 139, 165-177.

Pascual, A., and Preat, T. (2001). Localization of long-term memory within the *Drosophila* mushroom body. Science 294, 1115-1117.

Petrova, I.M., Lahaye, L.L., Martianez, T., de Jong, A.W., Malessy, M.J., Verhaagen, J., Noordermeer, J.N., and Fradkin, L.G. (2013). Homodimerization of the Wnt receptor DERAILED recruits the Src family kinase SRC64B. Mol Cell Biol 33, 4116-4127.

Sakurai, M., Aoki, T., Yoshikawa, S., Santschi, L.A., Saito, H., Endo, K., Ishikawa, K., Kimura, K., Ito, K., Thomas, J.B., et al. (2009). Differentially expressed Drl and Drl-2 play opposing roles in Wnt5 signaling during *Drosophila* olfactory system development. J Neurosci 29, 4972-4980.

Shimizu, K., Sato, M., and Tabata, T. (2011). The Wnt5/planar cell polarity pathway regulates axonal development of the *Drosophila* mushroom body neuron. J Neurosci 31, 4944-4954.

Shin, J.E., and DiAntonio, A. (2011). Highwire regulates guidance of sister axons in the *Drosophila* mushroom body. J Neurosci 31, 17689-17700.

Timofeev, K., Joly, W., Hadjieconomou, D., and Salecker, I. (2012). Localized netrins act as positional cues to control layer-specific targeting of photoreceptor axons in *Drosophila*. Neuron 75, 80-93.

Xu, K., Wu, Z., Renier, N., Antipenko, A., Tzvetkova-Robev, D., Xu, Y., Minchenko, M., Nardi-Dei, V., Rajashankar, K.R., Himanen, J., et al. (2014). Neural migration. Structures of netrin-1 bound to two receptors provide insight into its axon guidance mechanism. Science 344, 1275-1279.

Yao, Y., Wu, Y., Yin, C., Ozawa, R., Aigaki, T., Wouda, R.R., Noordermeer, J.N., Fradkin, L.G., and Hing, H. (2007). Antagonistic roles of Wnt5 and the Drl receptor in patterning the *Drosophila* antennal lobe. Nat Neurosci 10, 1423-1432.

Yoshikawa, S., Bonkowsky, J.L., Kokel, M., Shyn, S., and Thomas, J.B. (2001). The derailed guidance receptor does not require kinase activity *in vivo*. J Neurosci 21, RC119. Yoshikawa, S., McKinnon, R.D., Kokel, M., and Thomas, J.B. (2003). Wnt-mediated axon guidance via the *Drosophila* Derailed receptor. Nature 422, 583-588.

Yu, D., Akalal, D.B., and Davis, R.L. (2006). *Drosophila* alpha/beta mushroom body neurons form a branch-specific, long-term cellular memory trace after spaced olfactory conditioning. Neuron 52, 845-855.

Zhu, S., Lin, S., Kao, C.F., Awasaki, T., Chiang, A.S., and Lee, T. (2006). Gradients of the *Drosophila* Chinmo BTB-zinc finger protein govern neuronal temporal identity. Cell 127, 409-422.

SUPPLEMENTARY MATERIAL

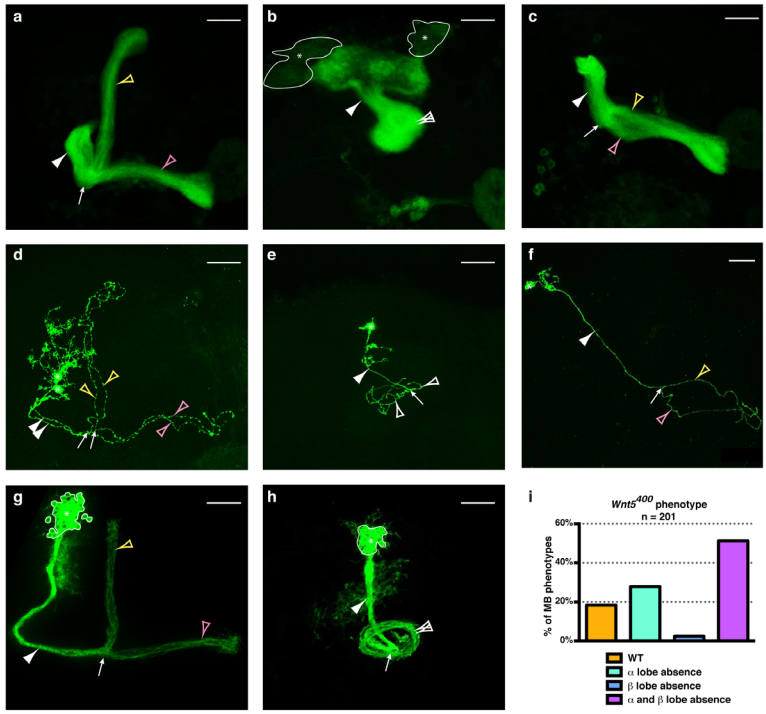

Figure S1, related to Figure 1. WNT5 is involved in α branch axon guidance

All the images shown are of *wnt5*^{null} individuals expressing *mGFP* driven by *c739-GAL4* to specifically label adult αβ neurons. An asterisk indicates the neuronal cell body, a white arrowhead and a white arrow represent the peduncle and the branch point, respectively. The α lobe or branch (yellow arrowhead) projects vertically and the β lobe or branch (pink arrowhead) projects toward the midline. (A, D, and G) In a *wnt5*^{null}, when total MBs are visualized 18% appear wild-type (A). As representative clones of this wild-type class; a two-cell clone (D) and a multiple cell clone (G) are shown. (B, E, and H) 51% of the MBs display a ball-shaped phenotype (B), due to the misguidance of both the α and β axons (empty white arrowhead) as shown in a single neuron clone (E) or in a multiple cell clone (H). In this class, β branch axons were also misguided indicating that *wnt5*, possibly via another receptor than *drl,* might be involved in the β branch guidance. (C, F) 28% of the MBs lack the dorsal lobe (C) which is likely caused by misguidance of the α axons, as is shown in the single cell clone (F). Note that this panel is also presented as Figure 1E. (I) Graph representing the distribution of MB phenotypes in *wnt5*^{null} hemizygous males. Genotypes: (A, B, C, and I) *w*^{1118} *wnt5*^{400} *FRT19A/Y; c739-GAL4 UAS-mCD8GFP/+.* (D-H) *w*, hs-FLP, tubP-GAL80, wnt5*^{400} *FRT19A/w*^{1118} *wnt5*^{400} *FRT19A; c739-GAL4 UAS-mCD8GFP/UAS-mCD8GFP*. Scale bars represent 30 μm. Images are composite confocal stacks. See also Table S2.

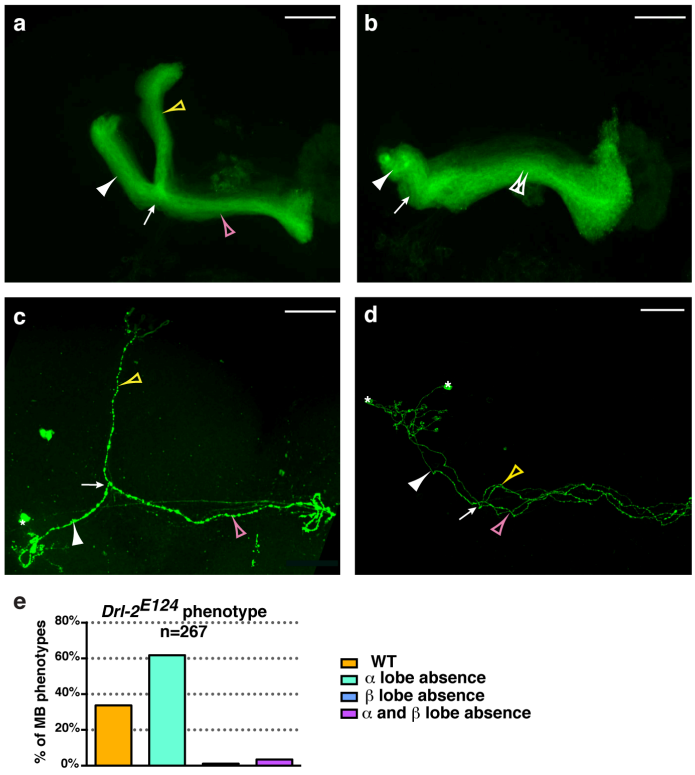

Figure S2, related to Figure 1. DRL-2 is involved in α branch axon guidance

All the MB neurons shown are from *drl-2^{null}* individuals. *GFP* expression driven by *c739- GAL4* specifically labels the adult αβ neurons. An asterisk indicates the neuronal cell bodies, a white arrowhead and a white arrow represent the peduncle and the branch point, respectively. In the *drl-2^{null}* mutant, ~ 34% of MBs appear wild-type when total MBs were visualized (A). A representative single cell clone of this class is shown (C). More than 60% of the MBs lack the dorsal lobe which is likely caused by α branch misguidance as is observed in a two-neuron clone (D). Note that this panel is also presented as Figure 1F. (E) Graph representing the distribution of MB phenotypes in *drl-2^{null}* individuals. Genotypes: (A, B, and E) *w^{1118}/y w 67c23; c739-GAL4 UAS-mCD8GFP, Drl-2^{E124}/Sp UAS-mCD8GFP, Df(2R)Exel8057*. (C and D) *w*, hs-FLP122, tubP-GAL80, FRT19A/w sn FRT19A; c739-GAL4 UAS-mCD8GFP, Drl- 2^{E124}/UAS-mCD8GFP, Df(2R)Exel8057*. Scale bars represent 30 μm. Images are composite confocal stacks. See also Table S2.

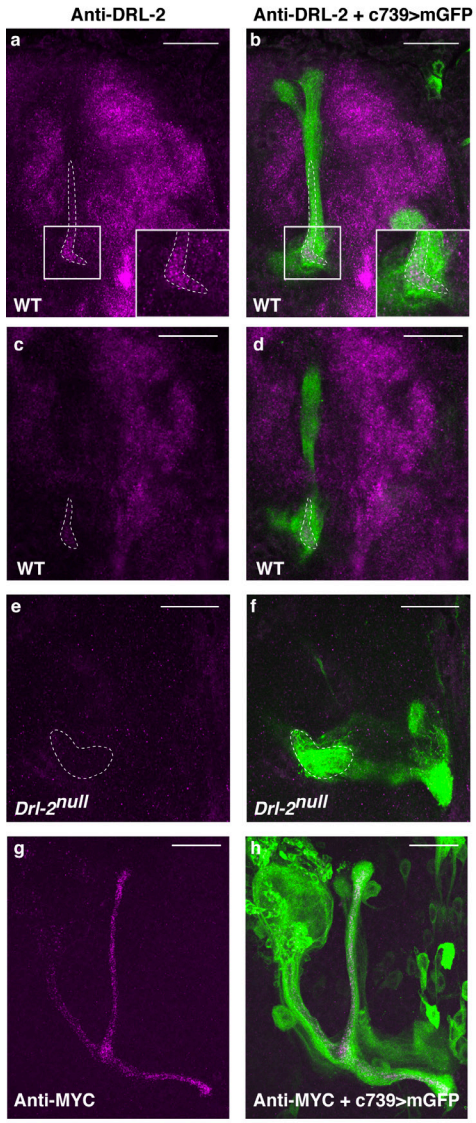

Figure S3, related to Figure 2. DRL-2 is expressed in the developing MB αβ neurons

All images shown are of 48 h APF *c739-GAL4 UAS-mCD8GFP* brains. DRL-2 (magenta) was expressed in the αβ axons (dotted area) of the wild-type MB (A, C). The overlap between MB neuron-expressed GFP (green) and DRL-2 is shown (B, D). Inserts in the lower right hand part of A and B panel show an enlargement of the area indicated in the main images by a white square. (E and F) 48 h APF *c739-GAL4 UAS-mCD8GFP drl-2^{null}* brain. DRL-2 was undetectable in a *drl-2^{null}* brain showing the specificity of the antibody. (G and H) 48 h APF *c739-GAL4 UAS-mCD8GFP; UAS-Drl-2-MYC* brains. MYC (magenta) was expressed in the αβ axons and MYC staining is apparently equivalent in the α and β branches. MYC expression is restricted to the core region and not in all of the GFP (green)-expressing αβ axons. This indicates that the DRL-2-MYC protein may be actively degraded and therefore is present only in the most recently extended axons. Genotypes: (A-D*) y w 67c23/y w 67c23; c739- GAL4 UAS-mCD8GFP/+*. (E and F) *y w^{67c23}/y w^{67c23}; c739-GAL4 UAS-mCD8GFP, Drl- 2^{E124}/Df(2R)Exel8057*. (G and H) *y w^{67c23}/y w^{67c23}; c739-GAL4 UAS-mCD8GFP/+; UAS-Drl- 2-MYC/+*. Scale bars represent 30 μm. Identical confocal settings were used in (A-F) images. Images are composite or single (C and D) confocal stacks.

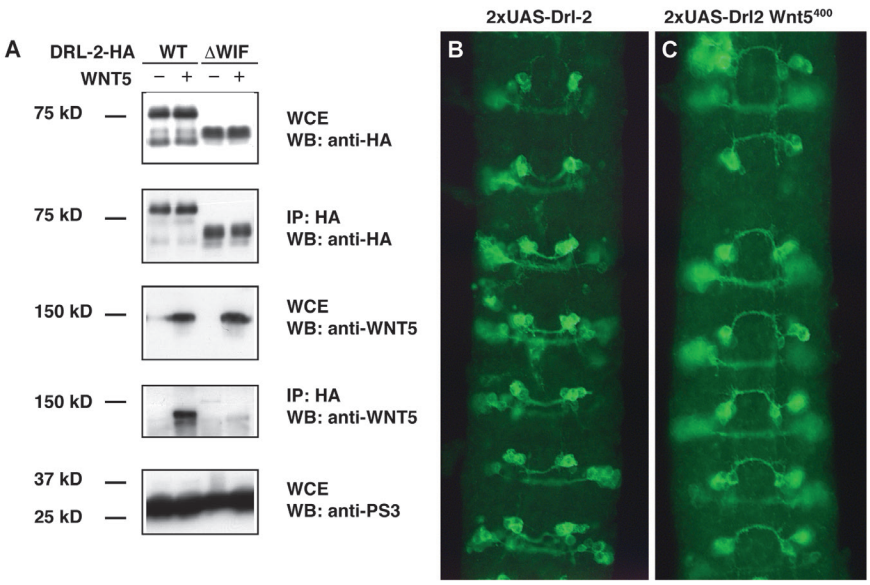

D

Genotype	% No switch	% Semi-switch	% Switch	n
2xUAS-Drl-2 / Y ; UAS-mCD8-GFP / + ; eg-GAL4 / +	0.5	6	93	376
2xUAS-Drl-2 Wnt5400 / Y ; UAS-mCD8-GFP / + ; eg-GAL4 / +	99	1	0	255

Figure S4, related to Figure 2. DRL-2 interacts with WNT5

(A) DRL-2 interacts with WNT5 via its WIF domain. *Drosophila* S2 cells were transiently transfected with the indicated expression constructs, lysates were immunoprecipitated (IP) with antibody specific to tagged DRL-2 (anti-HA) and subsequently immunoblotted (WB) with anti-WNT5 to detect co-immunoprecipitation of WNT5. Expression of DRL-2 and WNT5 was confirmed by immunoblotting of the whole cell extract (WCE). DRL-2 lacking its WIF domain (ΔWIF), unlike the wild-type receptor, does not interact with WNT5. (B-D) DRL-2 acts as a Wnt5-dependent axon repulsion receptor. Two copies of *UAS-Drl-2* in the wild-type (B) versus w*nt5*^{400} (C) backgrounds were driven by *eg-GAL4* in the presence of *UAS-mCD8-GFP* to visualize the *eg+* axons. Representative pictures and the quantitation (D) are shown.

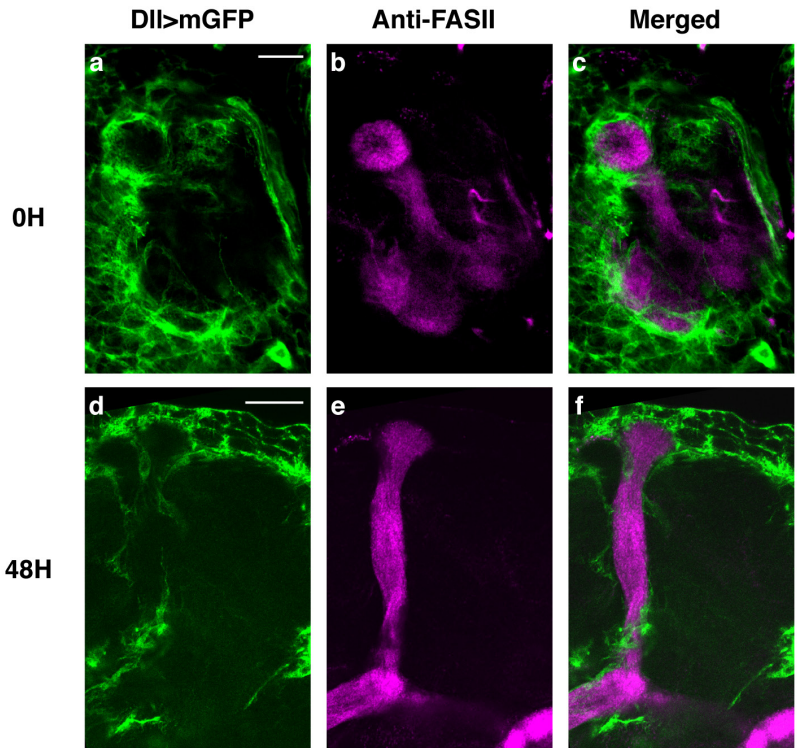

Figure S5, related to Figure 3. Close proximity of the Dll-GAL4 expressing neurons and the developing MBs

(A-C) 0 h APF brain *UAS-mCD8GFP Dll-GAL4* brain. (D-F) 48 h APF *UAS-mCD8GFP Dll-GAL4* brains. Green represents *Dll-GAL4* driven *GFP* and magenta corresponds to antibody against FASII showing the MB lobes. The spatial relationship between the *Dll-GAL4+* neurons and the MBs was examined from 0 hours to 48 hours APF brains and revealed a close proximity of the *Dll-GAL*-expressing neurons to the developing MBs. Genotype: *y* w^{67c23}*/y* w^{67c23}*; UAS-mCD8GFP Dll-GAL4 /+*. Scale bars represent 20 µm. Each image is a single confocal section.

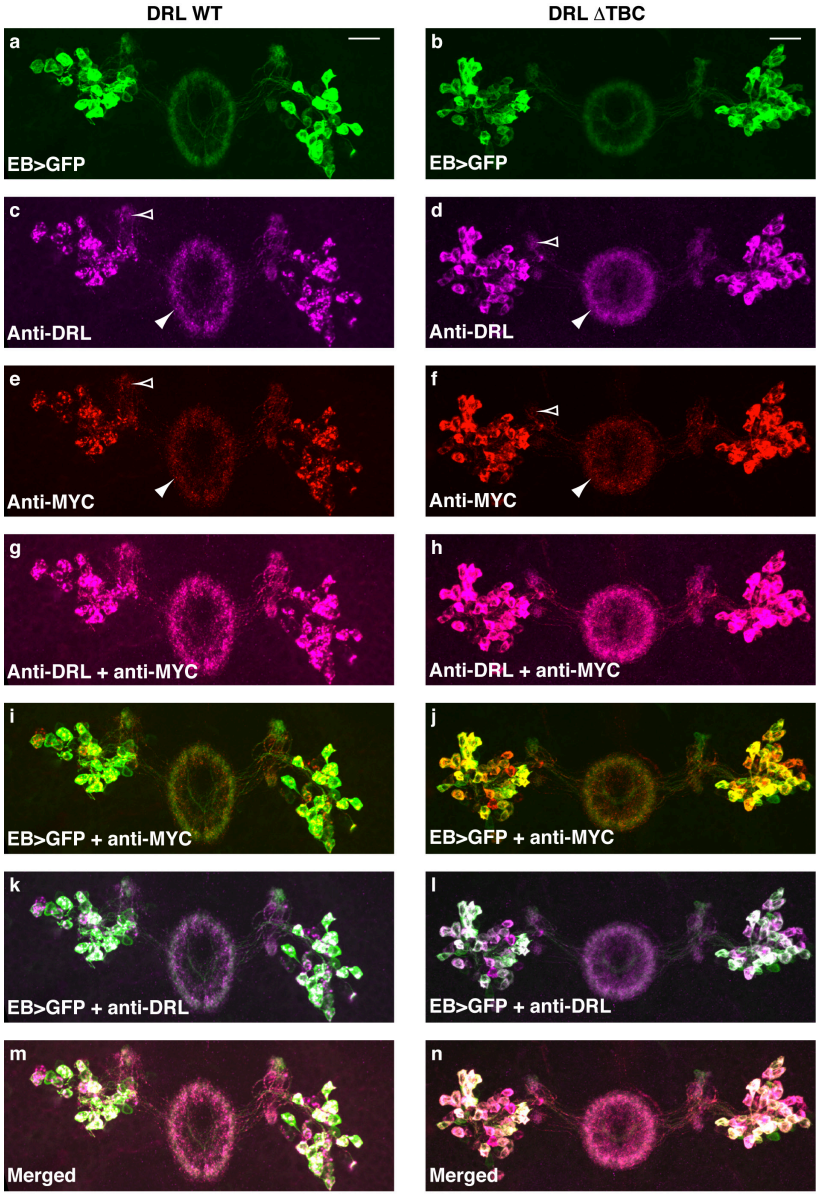

Figure S6, related to Figure 6. Sub-cellular specificity of *UAS-drlΔTBC-MYC* transgene expression

All images shown are of 48 h APF *drl^{null}, EB + c232-GAL4* brains. Green represents ellipsoid-body *GAL4*-driven *GFP* (*EB-GAL4 + c232-GAL4*), magenta indicates anti-DRL antibody and red corresponds to antibody against MYC. The stainings were done in a *drl^{null}* mutant background to avoid visualizing endogenous DRL expression. The ellipsoid body, which is not visibly affected by the lack of DRL, was used as a reference point for the localization of the transgene-driven proteins. The *UAS-drlΔTBC-MYC* transgene expression (B, D, F, H, J, L, and N) appeared very similar, if not identical, to that of the wild-type transgene (A, C, E, G, I, K, and M), either at the dendrite (empty arrowhead) or at the axon (arrowhead) levels. Genotypes: DRL WT: *UAS-drl WT-MYC/y w^{67c23}; drl^{R343}/lio^{2} UASmCD8GFP; (EB + c232)-GAL4/+*. DRL ΔTBC*: y w^{67c23}/y w^{67c23}; drl^{R343}/lio^{2} UASmCD8GFP; (EB + c232)-GAL4/2xUAS-drlΔTBC-MYC.* Scale bars represent 20 µm. Images are composite confocal sections

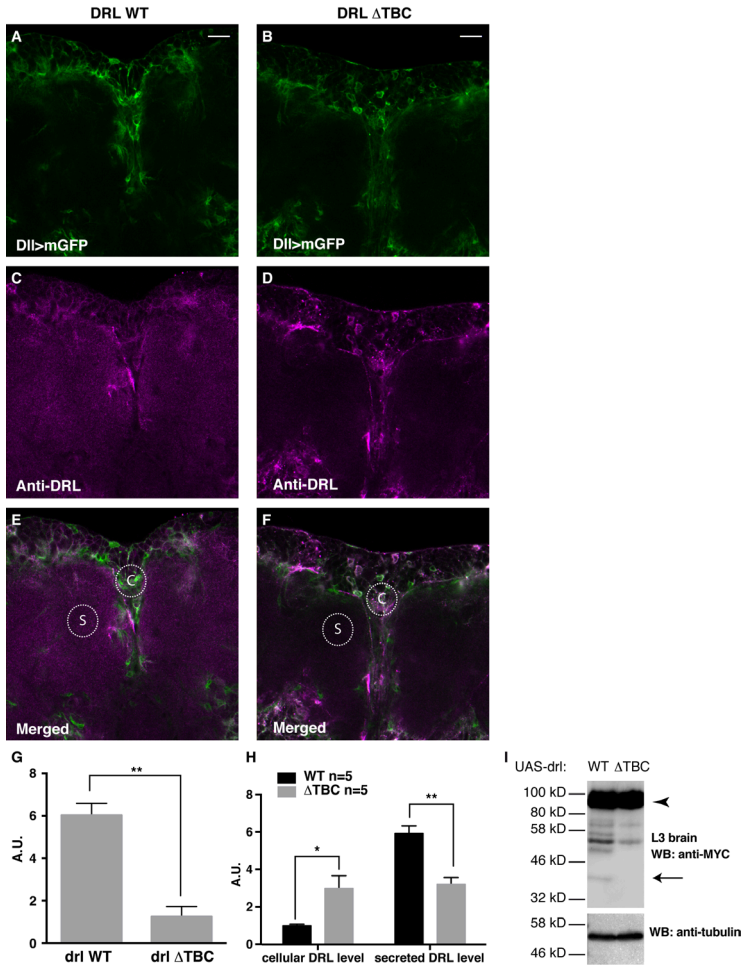

Figure S7, related to Figure 6. DRL ECD diffusion throughout the brain is significantly suppressed when the TBC site is mutated

(A-F) All images shown are of 48 h APF *drl*^{null} *UAS-mCD8GFP Dll-GAL4* brains. Green represents *Dll-GAL4*-driven GFP and magenta indicates anti-DRL antibody. (G) Ratio of the shed to cell membrane-associated DRL in *UAS-drl WT* (WT) compare to *UAS-drlΔTBC* (ΔTBC) calculated from the quantitation shown in (H) **: P < 0.01 (Wilcoxon rank sum test). (H) Quantitation of the intensity of the DRL signal in arbitrary units (A.U.). Intensity measurements of DRL were made with the Plot Profile tool of the FIJI software using identical settings for the two samples and normalized to GFP expression. Cell-associated DRL was measured in the region "C" and the shed DRL ECD in the region "S" shown in E and F. The data were subsequently analyzed using Prism software to calculate the means +/- SEM. n=5 brains analyzed in each case. There is more cell-associated DRL in the ΔTBC brain than in the WT brain because there are two ΔTBC and only one WT transgenes *: P < 0.05 (t test). Nevertheless, there is more secreted DRL in the WT brain than in the ΔTBC brain **: P < 0.01 (t test). Thus, DRL ECD diffusion from the DRL-expressing cells requires a wild-type TBC site. Genotypes: *UAS-drl WT-MYC/y w*^{67c23}*; drl*^{R343}*/lio*^{2} *UAS-mCD8GFP Dll-GAL4*. y *w*^{67c23}*/y w*^{67c23}*; drl*^{R343}*/lio*^{2} *UAS-mCD8GFP; Dll-GAL4; 2xUAS-drlΔTBCMYC/+*. (I) Western blot analysis of *elav-GAL4* L3 brain lysates (10 brains/lane) expressing either 2x*UAS-drl-Myc* (drl WT) or 2x*UAS-drlΔTBC-Myc* (drl ΔTBC). Anti-MYC revealed a dominant band of ~90 kD (arrowhead) and a small band of ~40 kD (arrow). The dominant band corresponds to full length DRL. The small band corresponds to the expected size of the carboxyterminal region of the protein liberated by cleavage at the TBC site present in drl WT but not in drl ΔTBC. Scale bars represent 20 μm. Images are composites of 10 confocal sections.

Table S1, related to Figure 1. Quantitation of neuroblast and 2-cell/single-cell clone phenotypes in the WT and *drl* mutant

Clones		WT	α mutant		α and β guidance	WT+ MLC	α mutant + MLC		β guidance	n=
			guidance	growth			guidance	growth		
WT	NB	78% 32	0% 0		0% 0	22% 9	0% 0		0% 0	41
	2/1-cell	90% 35	0% 0	0% 0	0% 0	10% 4	0% 0	0% 0	0% 0	39
***drl*^{null}**	NB	4% 1	22% 6		0% 0	0% 0	74% 20		0% 0	27
	2/1-cell	0% 0	6% 2	0% 0	0% 0	3% 1	91% 33	0% 0	0% 0	36
***drl*^{hypo}**	NB	57% 30	4% 2		0% 0	29% 15	10% 5		0% 0	52
	2/1-cell	34% 4	8% 1	8% 1	0% 0	42% 5	8% 1	0% 0	0% 0	12

WT: wild-type, NB: neuroblast clones, 2/1-cell: 2-cell/single-cell clones, MLC: midline crossing, n: number of clones analyzed. The number in blue in the lower right-hand corner of the cells corresponds to the number of clones analyzed in each category.

Table S2, related to Figure 1 and to Figures S1 and S2. Quantitation of neuroblast and 2-cell/single-cell clone phenotypes in WT, *drl*, *Wnt5* and *Drl-2* mutants

Clones		WT	[α] guidance	[α] growth	[α and β] guidance	[β] guidance	n=
WT	NB	100% 41	0% 0		0% 0	0% 0	41
	2/1-cell	100% 39	0% 0	0% 0	0% 0	0% 0	39
***drl*^{null}**	NB	4% 1	96% 26		0% 0	0% 0	27
	2/1-cell	3% 1	97% 35	0% 0	0% 0	0% 0	36
***Wnt5*^{null}**	NB	29% 5	47% 8		24% 4	0% 0	17
	2/1-cell	31% 15	26% 12	17% 8	26% 12	0% 0	47
***Drl-2*^{null}**	NB	25% 30	70% 83		3% 4	2% 2	119
	2/1-cell	42% 31	50% 37	5% 4	1.5% 1	1.5% 1	74

WT: wild-type, NB: neuroblast clones, 2/1-cell: 2-cell/single-cell clones, n: number of clones analyzed. The number in blue in the lower right-hand corner of the cells corresponds to the number of clones analyzed in each category. The WT and *drl*^{null} [α] numbers correspond to those in Table S1 under [α] and [α] + MLC but are here now pooled because MLC is not taken into account in this table.